

An improved method to calculate the directions and weights in microplane constitutive model

W. Cheng & Z. Shen

Tongji University, Shanghai 200092, P. R. China

ABSTRACT: In this paper, a new method to calculate the directions and weights in microplane constitutive model was proposed. The surface of a unit cube was divided into regular rectangle grids, and then microplanes were generated by mapping those grids onto a unit spherical surface, of which each microplane was a spherical quadrilateral. The directional vector of a microplane will be determined by the central point of the related rectangle on the cubic surface, and the functions for calculating the microplane weight were derived by means of spherical geometry theory. A non-uniform indicator to analyze the non-uniformity of the distributed microplanes was established. It was shown that the distribution of the microplanes was non-uniform when the surface of cube was meshed uniformly. However the non-uniformity of the distributed microplanes would be improved greatly when the grids of cube surface were configured properly.

KEY WORDS: constitutive model, microplane, spherical geometry, non-uniformity, weight

1 INTRODUCTION

Concrete is a kind of composite material which was combined by cement mortar and coarse granule with different diameters. For several decades, constitutive models for concretes have been greatly concerned by structural engineers, and a lot of engineering practices have shown that an appropriate constitutive model of concrete is crucial for describing the complex mechanical behavior in structures. Until now, the constitutive models for concrete material proposed by researchers can be divided into two categories as: (1) the macro phenomenological models, (2) the models based on micro-mechanics.

The macro phenomenological models include: the elastic mechanics models, the plastic mechanics models, endochronic models, and the models based on damage and fracture mechanics theory. Although the researchers have achieved a series of success and made a great development and progress using this kind of constitutive models^[1], there still exist limitations for macro phenomenological models to describe the complex properties of concrete which can be summarized as follows:

- (1) For those concise models, it is difficult to fully embody the mechanical properties of concrete, such as yielding, cracking, hysteresis, softening, and etc.
- (2) For those complicated models, there may exist difficulties in determining unknown parameters, and the formulas are so fussy that the amount of computation will be considerably large, and

there will even exist problems like instability and non-convergence in computation.

- (3) Sometimes the yielding surface is not smooth, which may consequently lead to the problem of singularity in calculation.
- (4) The stress-strain relationship can hardly be harmonious with the yielding surface and fracture criterion.
- (5) The ideal approaches to deal with general anisotropies of concrete material are scarce. It causes to the dilemma in describing nonlinear behaviors of concrete due to damage and fracture.
- (6) As the increasing of testing data storage of concrete, it is extremely difficult to find a generally accepted constitutive model with one set of material parameters which can be used to simulate the responses of material under different loadings.

In 1938, Taylor proposed the micro constitutive model for polycrystalline metals^[2]. The relationship between the components of micro-stress and the components of micro-strain in any direction was established. And based on the kinematic-static constrains between macroscopic and microscopic quantities, and the deformation energy Equation, the macro stress-strain relationship was obtained. The essence of this method is that the macro stresses and the constitutive relationship matrices can be calculated by integrating the contributions of all micro-structures. Bazant and his cooperators, who enlightened by the idea of Taylor, improved the

theory of plastic slip and extended it to concrete, and proposed the microplane model which can describe the behavior of micro-cracking of concrete. Some literatures^[3-7] show that the microplane model is effective to simulate the nonlinear mechanical properties of concrete.

Compared with the classical macro constitutive models based on invariants of stress or strain tensor, the advantages of microplane are obvious, as:

- (1) As Taylor was aware in 1938, the micro constitutive model is more clarity in form, more concise in concept and easier to manipulate than the macro ones.
- (2) The stress-component functions of strain-component in microplanes, can be directly used to describe the deformational and mechanical properties in specific directions. However, for macro constitutive models, it is incapable to exhibit friction, slip or local cracking properties on planes in specific directions using functions of macro strain-tensor, hydrostatic pressure and second-order deviatoric stress invariant, etc.
- (3) Rather different from macro plastic constitutive models, the plastic microplane model is equivalent to a large amount of active yielding surfaces and each one is determinate in form.
- (4) The loading-unloading states of all microplanes may be diverse, and it will be useful to exhibit complex path-dependent characteristics of materials as Bauschinger effect, hysteretic effect, softening effect and so on under cyclic loading.
- (5) The overall fatigue degree can be simulated by integrating those of all microplanes.
- (6) At last, the material anisotropy can be described by the microplanes in all directions.

The main disadvantage of microplane model is that a huge amount of computation will be needed. However it can be expected that this disadvantage will become insignificant as computing capability being enhanced continuously.

It is very important, in microplane constitutive theory, to dispose microplanes properly for better computational accuracy and efficiency. Bažant etc.^[8] conducted a special research on it. Several fixed points on the surface of a regular polyhedron were selected to represent the directions of microplanes, and then the weights of all microplanes were calculated through optimal method. The advantages and disadvantages of this method will be discussed later in this paper, and a new improved method, which based on mapping grids on the surface of a unit cube onto a unit sphere surface, will be constructed. The computing formulas for the new method are derived based on the theory of spherical geometry. And then it is implemented to indicate correctly the non-uniformity of the distribution of microplanes by introducing a non-uniform indicator

of microplanes. At last, a more ideal distribution of microplanes is obtained through the method of non-uniform grid division on cubic surface.

2 BASIC THEORY OF THE MICROPLANE CONSTITUTIVE MODEL

2.1 Basic hypotheses

The microplane constitutive theory is based on the plastic slip theory of Taylor, it assumes that the constitutive model can be determined by the stress-component functions of strain-component on a plane in any direction, and the plane is called microplane. The stress-components acting on the microplane are called micro-stresses and the strain-components as the counterparts of the micro-stresses are called micro-strains.

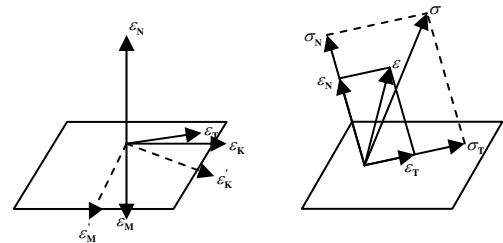


Figure 1. The stress-components and strain-components on a microplane.

Microplanes in different directions will act with each other, the theory of plastic slip assumes that the micro-strains can be expressed as a function of macro-strain tensor, thus the action between microplanes can be canceled out. However, two basic hypotheses are introduced with microplanes.

Hypothesis 1: the cracking behavior of concrete material can be described by normal micro-strain,

$$\varepsilon_N = n_i n_j \varepsilon_{ij} \quad (1)$$

in which, ε_N is the normal micro-strain, ε_{ij} is the macro-strain tensor, and $\mathbf{n} = (n_1, n_2, n_3)$ is the unit normal vector of the related microplane.

Hypothesis 2: the micro-stress is defined as function of the related micro-strain, i.e.

$$\sigma_N = \frac{2\pi}{3} F(\varepsilon_N) \quad (2)$$

here, σ_N is the normal micro-stress, $\frac{2\pi}{3}$ is the related normal micro-strain and factor 3 is for the purpose of convenience of laconic type in deriving.

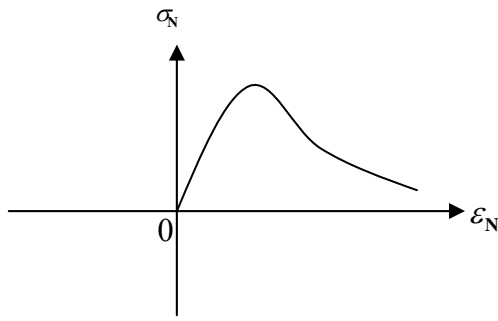


Figure 2. The curve of normal micro-stress and micro-strain.

2.2 Some other types of micro-strain and micro-stress

The conceptions of shear micro-stress (micro-strain), volumetric stress (strain) and deviatoric micro-stress (micro-strain) are also established in literatures^[4,5]. Further more, the functional relations between micro-stresses and micro-strains are also given, such as in Equation (3)-(8). Let

$$\varepsilon_V = \frac{\varepsilon_{11} + \varepsilon_{22} + \varepsilon_{33}}{3} \quad (3)$$

be the volumetric strain. Then the deviatoric micro-strain can be defined as

$$\varepsilon_D = \varepsilon_N - \varepsilon_V \quad (4)$$

and the shear micro-strains can be also defined as

$$\begin{cases} \varepsilon_L = L_{ij} \varepsilon_{ij} \\ \varepsilon_M = M_{ij} \varepsilon_{ij} \end{cases} \quad (5)$$

in which, L_{ij} and M_{ij} both are the products of two direction cosines. Suppose volumetric stress can be expressed via the volumetric strain as

$$\sigma_V = C_V(\varepsilon_V) \varepsilon_V \quad (6)$$

in which, C_V is the volumetric elastic modulus which is the function of volumetric strain. Similarly the deviatoric micro-stress is with form as

$$\sigma_D = C_D(\varepsilon_D) \varepsilon_D \quad (7)$$

here, C_D is the deviatoric elastic modulus which is the function of deviatoric micro-strain. And the shear micro-stress can be expressed as

$$\sigma_T = C_T(\varepsilon_T, \sigma_C) \varepsilon_T \quad (8)$$

in above Equation, C_T is the shear elastic modulus which is the function of shear micro-strain and the first stress invariant.

Formula (6), (7) and (8) can be used to describe more complex nonlinear mechanical behavior of concrete^[2-5]. At the later discussion in this paper, only the influence of the normal micro-stresses and normal micro-strains is considered for no other reason than that this paper is only concerning on the discrete method of microplanes and the calculation of directions and weights of them.

2.3 The integral formula of macro-stress

The macro-stress can be shown as:

$$\sigma_{ij} = \int_S F(\varepsilon_N) n_i n_j w(\mathbf{n}) dS \quad (9)$$

in which, S denotes for a half surface area of a unit sphere, dS is surface element and $w(\mathbf{n})$ is the orientational distribution function of direction \mathbf{n} . Usually the material is considered as isotropic, which leads to $w(\mathbf{n}) \equiv 1$.

Formula (9) gives the relation between micro-stresses and macro-stress through the principle of virtual work. The essence of this method is to transform the macro-problem to micro-scale and to obtain macro-stress through micro-stress function which is simply defined in micro-scale.

2.4 The integral formula of the macro tangent stiffness matrix

The macro tangent stiffness matrix can be expressed as^[1]:

$$D_{ijkm}^c = \int_S F'(\varepsilon_N) \alpha_{ijkm} dS \quad (10)$$

here, $F'(\varepsilon_N)$ is derivative of $F(\varepsilon_N)$ with respect to ε_N , and the forth-order tensor $\alpha_{ijkm} = n_i n_j n_k n_m$.

Deriving the macro tangent stiffness matrix is for the convenience of numerical calculation in finite element analysis.

2.5 The parameterized integral formula

Substituting the integral parameters with spherical coordinates (θ, ϕ) in formula (9) and (10), the double integral formulas can be obtained as

$$\sigma_{ij} = \int_0^{2\pi} \int_0^{\frac{\pi}{2}} F(\varepsilon_N) n_i n_j \sin \phi d\theta d\phi \quad (11)$$

And

$$D_{ijkm}^c = \int_0^{2\pi} \int_0^{\frac{\pi}{2}} F'(\varepsilon_N) \alpha_{ijkm} \sin \phi d\theta d\phi \quad (12)$$

3 DISCRETIZATION OF INTEGRAL AREA

3.1 The discretization of integral

Discretizing the integral area of (9) and (10), then two numerical expressions

$$\sigma_{ij} \approx \sum_{\alpha=1}^N \omega_{\alpha} [F(\varepsilon_N) n_i n_j]_{\alpha} \quad (13)$$

And

$$D_{ijkm}^c \approx \sum_{\alpha=1}^N \omega_{\alpha} [\alpha_{ijkm} F'(\varepsilon_N)]_{\alpha} \quad (14)$$

will be obtained, in which, N is the number of microplanes, α denotes the α -th microplane and ω_{α} is its weight.

3.2 The discrete methods in paper^[3-7]

In literature [8], the discrete method of spherical surface was investigated systematically, and the basic idea is to select some fixed points located on the surface of regular polyhedron to denote the directions of microplanes, and then to calculate the weights of all microplanes using optimal approach. The advantages of this method are:

- (1) Those fixed points determined on surface of regular polyhedron have the virtue of being visual and distinct geometrically, so that it is convenient to grasp the directions of the material mechanical behavior such as yielding and cracking.
- (2) The weights of microplanes are calculated by optimal method, this assure that high precision can be obtained under common loading.
- (3) There exists a symmetric plane with all integration points on spherical surface, sometimes even orthogonality can be satisfied.
- (4) The data of directions and the weights of microplanes can be calculated beforehand that is beneficial for the design of program.

disadvantages of this method, however, are:

- (1) Since the shape of a microplane is not clear, the area covered by the microplane is indistinct.
- (2) The distribution of all microplanes is non-uniform, it may cause the accuracy loss, especially when the microplanes experience diversely.
- (3) The calculation for weights is so complex that any refinement for the discretization is hard.

4 THE IMPROVEMENT OF THE METHOD OF DISCRETIZING THE INTEGRAL AREA

4.1 Discretization of spherical coordinate parameters

It is convenient to adopt the spherical coordinate to express the integral area as

$$0 \leq \theta \leq 2\pi, 0 \leq \varphi \leq \frac{\pi}{2} \quad (15)$$

here, θ and φ are longitude and latitude respectively, then the formula (10) can be expressed as:

$$D_{ijkm}^c = \int_0^{2\pi} d\theta \int_0^{\frac{\pi}{2}} F'(\varepsilon_N) \alpha_{ijkm} \sin \phi d\phi \quad (16)$$

The deflection of this discretization method is that the non-uniformity still exists, but when the deformations of concrete satisfy axial symmetry (such as uniaxial loading) the calculation efficiency may be high.

4.2 Cubic grid mapping

4.2.1 The uniform discretization of cubic surface

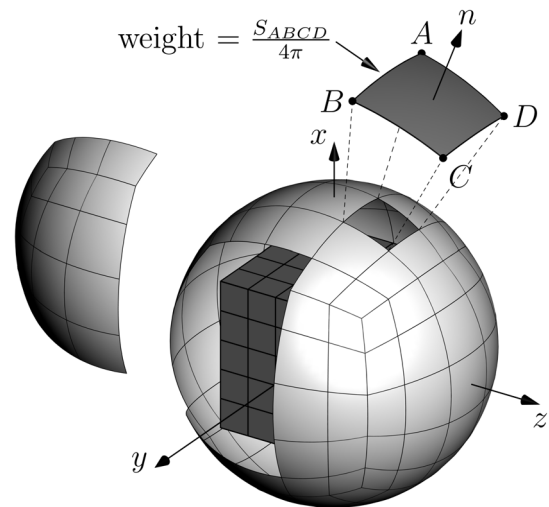


Figure 3. The figure of discrete cube and projection*.

Shown in Figure 2, there is a unit sphere and a cube, the sphere and the cube have the same center, the cube can be expressed conveniently as:

$$-1 \leq x, y, z \leq 1$$

There are 6 surfaces on the cube, which can be expressed as:

*In practical situation the cubic surface should circumscribe around the unit sphere, there, for the sake of expressing the mapping relation clarity, draw the cube within the sphere, it can be comprehended as their length-units are different in size.

$$\hat{\Gamma}_{x=\pm 1} : x = \pm 1, -1 \leq y, z \leq 1$$

$$\hat{\Gamma}_{y=\pm 1} : y = \pm 1, -1 \leq x, z \leq 1$$

$$\hat{\Gamma}_{z=\pm 1} : z = \pm 1, -1 \leq x, y \leq 1$$

Because the integral area of formula (9) and (10) is semi-spherical surface, so it is only needed to made uniform meshes on the cubic surfaces with normal directions same as coordinate axes. For instance, the surface $\Gamma_{x=1}$ can be meshed as Figure 4.

The nodes coordinates of the grid are expressed as:

$$\hat{r}_{ij} = \left(1, -1 + \frac{2i}{k}, -1 + \frac{2j}{k} \right) \quad (i, j = 0, 1, \dots, k) \quad (17)$$

For the other 2 surfaces $\hat{\Gamma}_{y=1}$ and $\hat{\Gamma}_{z=1} \lim_{x \rightarrow \infty}$, the meshes and nodes can be obtained similarly.

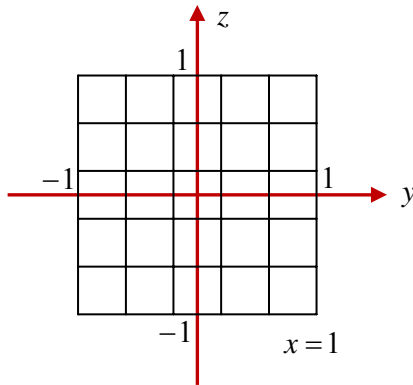


Figure 4. The uniform meshes of cubic surface $x = 1$.

4.2.2 Mapping the uniform grid on the cubic surface onto the unit spherical surface

The unit spherical surface will be discretized by mapping the grid on the cubic surface onto the unit spherical surface (Fig. 3), so that a series of small mapped spherical quadrilaterals will be generated, of which each small mapped area gives a microplane. The direction of a microplane is the radius vector from the origin to the center of the related small square, and the weight (shown in Fig. 3) is equal to the ratio of the area of the small spherical quadrilateral to the unit spherical area 4π .

Now mapping the points of formula (17) onto the unit spherical surface results in

$$r_{ij} = \frac{\hat{r}_{ij}}{|\hat{r}_{ij}|} \quad (18)$$

Similarly, all the coordinates of the nodes on the cubic surface $\hat{\Gamma}_{y=1}$ and $\hat{\Gamma}_{z=1}$ and the mapping points' coordinates on the unit spherical surface can be calculated in same way.

4.2.3 The directions and weights of the microplanes

Using the surface of $x=1$ as a sample to give the formulas to calculate directions and weights.

4.2.4 The directions of the microplanes

The center coordinates of small quadrilaterals on the cubic surface are:

$$\hat{n}_{ij} = \frac{\hat{r}_{ij} + \hat{r}_{i,j+1} + \hat{r}_{i+1,j} + \hat{r}_{i+1,j+1}}{4} = \left(1, -1 + \frac{2i+1}{k}, -1 + \frac{2j+1}{k} \right) \quad (i, j = 0, 1, \dots, k-1) \quad (19)$$

mapping them onto the surface of unit sphere, the unit normal direction of the related microplane can be obtained as:

$$n_{ij} = \frac{\hat{n}_{ij}}{|\hat{n}_{ij}|}, \quad (i, j = 0, 1, \dots, k-1) \quad (20)$$

4.2.5 The weights of the microplanes

In Figure 3, assuming that the spherical quadrilateral $ABCD$ is a microplane, here the coordinates of points A, B, C and D is $r_{ij}, r_{i+1,j}, r_{i+1,j+1}$ and $r_{i,j+1}$ respectively. Denote the area of the spherical quadrilateral $ABCD$ as $S_{ij} = S_{ABCD} = S_{r_{ij}r_{i+1,j}r_{i+1,j+1}r_{i,j+1}}$, then the weight of this microplane will be

$$\omega_{ij} = \frac{S_{ij}}{4\pi} \quad (21)$$

here, ω_{ij} is the weight of the microplane corresponding to the double-subscript (i, j) . Accordingly, calculating the weight of the microplane depends on computing the area of the spherical quadrilateral.

4.2.6 Calculating the area of the spherical quadrilateral

From the theory of spherical geometry^[9], it can be known that the area of spherical quadrilateral is:

$$S_{ij} = S_{ABCD} = A + B + C + D - 2\pi \quad (22)$$

here, A, B, C and D are the interior angles of spherical quadrilateral $ABCD$.

Let P and Q be the arbitrary 2 points on a unit spherical surface, and l_{PQ} ($l_{PQ} \leq \pi$) denote the arc-length of great circle. Then

$$\begin{cases} \cos l_{AB} = \cos l_{BA} = r_{ij} \cdot r_{i+1,j} \\ \cos l_{AC} = \cos l_{CA} = r_{ij} \cdot r_{i+1,j+1} \\ \cos l_{AD} = \cos l_{DA} = r_{ij} \cdot r_{i,j+1} \\ \cos l_{BC} = \cos l_{CB} = r_{i+1,j} \cdot r_{i+1,j+1} \\ \cos l_{BD} = \cos l_{DB} = r_{i+1,j} \cdot r_{i,j+1} \\ \cos l_{CD} = \cos l_{DC} = r_{i+1,j+1} \cdot r_{i,j+1} \end{cases} \quad (23)$$

and

$$\left\{ \begin{array}{l} \sin l_{AB} = \sin l_{BA} = |r_{ij} \times r_{i+1,j}| \\ \sin l_{AC} = \sin l_{CA} = |r_{ij} \times r_{i+1,j+1}| \\ \sin l_{AD} = \sin l_{DA} = |r_{ij} \times r_{i,j+1}| \\ \sin l_{BC} = \sin l_{CB} = |r_{i+1,j} \times r_{i+1,j+1}| \\ \sin l_{BD} = \sin l_{DB} = |r_{i+1,j} \times r_{i,j+1}| \\ \sin l_{CD} = \sin l_{DC} = |r_{i+1,j+1} \times r_{i,j+1}| \end{array} \right. \quad (24)$$

will be derived. Using the following spherical law of cosines

$$\left\{ \begin{array}{l} \sin l_{AD} \sin l_{AB} \cos A = \cos l_{BD} - \cos l_{AD} \cos l_{AB} \\ \sin l_{BC} \sin l_{AB} \cos B = \cos l_{CA} - \cos l_{BC} \cos l_{AB} \\ \sin l_{CD} \sin l_{BC} \cos C = \cos l_{DB} - \cos l_{CD} \cos l_{BC} \\ \sin l_{CD} \sin l_{AD} \cos D = \cos l_{AC} - \cos l_{CD} \cos l_{AD} \end{array} \right. \quad (25)$$

then all interior angles can be obtained as

$$\left\{ \begin{array}{l} A = \arccos \frac{\cos l_{BD} - \cos l_{AD} \cos l_{AB}}{\sin l_{AD} \sin l_{AB}} \\ B = \arccos \frac{\cos l_{CA} - \cos l_{BC} \cos l_{AB}}{\sin l_{BC} \sin l_{AB}} \\ C = \arccos \frac{\cos l_{DB} - \cos l_{CD} \cos l_{BC}}{\sin l_{CD} \sin l_{BC}} \\ D = \arccos \frac{\cos l_{AC} - \cos l_{CD} \cos l_{AD}}{\sin l_{CD} \sin l_{AD}} \end{array} \right. \quad (26)$$

Substituting Equations (26) into (22), the area of spherical quadrilateral can be obtained. And using formula (21), the weights of the microplanes on the sphere $\Gamma_{x=1}$ can be calculated then.

Table 1. The directional cosines and the weights of 21 microplanes^[3].

α	n_1^α	n_2^α	n_3^α	ω_a
1	0.1876	0.0000	0.0000	0.0198
2	0.7947	-0.5257	-0.5257	0.0198
3	0.7947	0.5257	0.5257	0.0198
4	0.1876	-0.8507	-0.8507	0.0198
5	0.7947	0.0000	0.0000	0.0198
6	0.1876	0.8507	0.8507	0.0198
7	0.5774	-0.3090	-0.3090	0.0254
8	0.5774	0.3090	0.3090	0.0254
9	0.9342	0.0000	0.0000	0.0254
10	0.5774	-0.8090	-0.8090	0.0254
11	0.9342	-0.3090	-0.3090	0.0254
12	0.9342	0.3090	0.3090	0.0254
13	0.5774	0.8090	0.8090	0.0254
14	0.5774	-0.5000	-0.5000	0.0254
15	0.5774	0.5000	0.5000	0.0254
16	0.3568	-0.8090	-0.8090	0.0254
17	0.3568	0.0000	0.0000	0.0254
18	0.3568	-0.8090	-0.8090	0.0254
19	0.0000	-0.5000	-0.5000	0.0254
20	0.0000	-0.5000	-0.5000	0.0254
21	0.0000	1.0000	1.0000	0.0254

Now, present the directional cosines and the weights of 21 microplanes given in reference [3] in Table 1.

Then, calculate the directional cosines and weights of the microplanes via the formulas (21), (22) and (26), and show the results in Table 2 and Table 3, the discrete number is chosen as $k = 3$ and $k = 5$ respectively.

Table 2. The directional cosines and weights of 27 microplanes with $k = 3$.

α	n_1^α	n_2^α	n_3^α	ω_a
1	0.7276	-0.4851	-0.4851	0.0137
2	0.8321	-0.5547	0.0000	0.0199
3	0.7276	-0.4851	0.4851	0.0137
4	0.8321	0.0000	-0.5547	0.0199
5	1.0000	0.0000	0.0000	0.0319
6	0.8321	0.0000	0.5547	0.0199
7	0.7276	0.4851	-0.4851	0.0137
8	0.8321	0.5547	0.0000	0.0199
9	0.7276	0.4851	0.4851	0.0137
10	-0.4851	0.7276	-0.4851	0.0137
11	0.0000	0.8321	-0.5547	0.0199
12	0.4851	0.7276	-0.4851	0.0137
13	-0.5547	0.8321	0.0000	0.0199
14	0.0000	1.0000	0.0000	0.0319
15	0.5547	0.8321	0.0000	0.0199
16	-0.4851	0.7276	0.4851	0.0137
17	0.0000	0.8321	0.5547	0.0199
18	0.4851	0.7276	0.4851	0.0137
19	-0.4851	-0.4851	0.7276	0.0137
20	-0.5547	0.0000	0.8321	0.0199
21	-0.4851	0.4851	0.7276	0.0137
22	0.0000	-0.5547	0.8321	0.0199
23	0.0000	0.0000	1.0000	0.0319
24	0.0000	0.5547	0.8321	0.0199
25	0.4851	-0.4851	0.7276	0.0137
26	0.5547	0.0000	0.8321	0.0199
27	0.4851	0.4851	0.7276	0.0137

Table 3. The directional cosines and weights of 75 microplanes with $k = 5$.

α	n_1^α	n_2^α	n_3^α	ω_a
1	0.6623	-0.5298	-0.5298	0.0037
2	0.7454	-0.5963	-0.2981	0.0053
3	0.7809	-0.6247	0.0000	0.0061
4	0.7454	-0.5963	0.2981	0.0053
5	0.6623	-0.5298	0.5298	0.0037
6	0.7454	-0.2981	-0.5963	0.0053
7	0.8704	-0.3482	-0.3482	0.0083
8	0.9285	-0.3714	0.0000	0.0100
9	0.8704	-0.3482	0.3482	0.0083
10	0.7454	-0.2981	0.5963	0.0053
11	0.7809	0.0000	-0.6247	0.0061
12	0.9285	0.0000	-0.3714	0.0100
13	1.0000	0.0000	0.0000	0.0122
14	0.9285	0.0000	0.3714	0.0100
15	0.7809	0.0000	0.6247	0.0061
16	0.7454	0.2981	-0.5963	0.0053
17	0.8704	0.3482	-0.3482	0.0083
18	0.9285	0.3714	0.0000	0.0100
19	0.8704	0.3482	0.3482	0.0083
20	0.7454	0.2981	0.5963	0.0053

21	0.6623	0.5298	-0.5298	0.0037
22	0.7454	0.5963	-0.2981	0.0053
23	0.7809	0.6247	0.0000	0.0061
24	0.7454	0.5963	0.2981	0.0053
25	0.6623	0.5298	0.5298	0.0037

*Only the data of the microplanes on the surface $\Gamma_{x=1}$ are presented here, however the data of the microplanes on the surfaces $\Gamma_{y=1}$ and $\Gamma_{z=1}$ can be obtained by replacing the directional coordinates.

4.2.7 *The non-uniform indicator of the microplanes*
Now define a non-uniform indicator of the microplanes as:

$$\lambda_N = \frac{\max_{\alpha=1}^N \omega_\alpha - \min_{\alpha=1}^N \omega_\alpha}{\min_{\alpha=1}^N \omega_\alpha} \times 100\% \quad (27)$$

The larger λ_N is, the more prominent the non-uniformity is. If λ_N approaches 0, the distribution of the microplanes will tend towards uniform. Calculate the non-uniform indicators for Table 1, Table 2 and Table 3 respectively, it can be noticed that the non-uniform indicator for Table 1 is 25.8%, however, for Table 2 ($k=3$) and Table 3 ($k=5$), the non-uniform indicators are 132.85% and 229.73%, respectively.

It can be seen that the above results are not ideal. The main reason causing so large non-uniform indicators is that the discrete method used here is mapping the uniform meshes of the cubic surface onto the unit spherical surface. Indeed the ratio of any two rectangles on cubic surface is equal to 1, however when mapping them onto the unit sphere, the closer a microplane approaches to axial of the coordinate-system, the smaller its area is. Hence the uniformity of microplanes distribution decreases. This shortcoming can be improved by using non-uniform grid on cubic surface.

5 NON-UNIFORM MESH METHOD

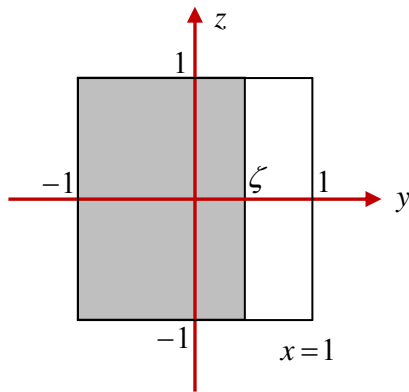


Figure 5. Mapping the shadow area to the unit sphere.

The shadow area on the cubic surface (Fig. 5) is

$$x = 1, \quad -1 \leq y \leq \zeta, \quad -1 \leq z \leq 1.$$

Mapping it onto the unit sphere. The image area on the spherical surface can be derived using formula (22) as

$$S(\zeta) = \frac{\pi}{3} + 2 \arcsin \frac{\zeta}{\sqrt{2(1+\zeta^2)}}, \quad -1 \leq \zeta \leq 1 \quad (28)$$

Now try to find a finite sequence $0 < \zeta_1 < \dots < \zeta_m = 1$, to satisfy

$$\begin{cases} S(\zeta_{i+1}) - S(\zeta_i) = \frac{2\pi}{3(2m-1)}, & i=1,2,\dots,m-1 \\ S(\zeta_1) - S(0) = \frac{\pi}{3(2m-1)} \end{cases} \quad (29)$$

It implies that the unit square is divided into a series of rectangular strips, when mapping them onto the spherical surface, the area of each spherical quadrilateral strip is same. Thus

$$\zeta_i = \sqrt{\sec\left(\frac{2i-1}{2m-1} \cdot \frac{\pi}{3}\right) - 1} \quad i=1,2,\dots,m \quad (30)$$

Then adopt

$$\eta_i = \begin{cases} -\zeta_{m-i}, & i=0,1,\dots,m-1 \\ \zeta_{i-m+1}, & i=m,m+1,\dots,k \end{cases} \quad (31)$$

as mesh points, here $k=2m-1$, then every rectangular strip on the surface of cube as

$$x = 1, \quad \eta_{i-1} \leq y \leq \eta_i, \quad -1 \leq z \leq 1 \quad (i=1,2,\dots,2m-1)$$

will be mapped onto the surface of the unit sphere with equal area. The motivation to do so is to make the microplanes with an approximately equal area and consequently to improve the uniformity of the distribution.

Table 4. The results of non-uniform division (27 microplanes).

α	n_1^α	n_2^α	n_3^α	ω_α
1	0.7484	-0.4690	0.4690	0.0187
2	0.8474	-0.5310	0.0000	0.0182
3	0.7484	-0.4690	0.4690	0.0187
4	0.8474	0.0000	-0.5310	0.0182
5	1.0000	0.0000	0.0000	0.0192
6	0.8474	0.0000	0.5310	0.0182
7	0.7484	0.4690	-0.4690	0.0187
8	0.8474	0.5310	0.0000	0.0182
9	0.7484	0.4690	0.4690	0.0187
10	0.4690	0.7484	-0.4690	0.0187
11	0.0000	0.8474	-0.5310	0.0182
12	0.4690	0.7484	-0.4690	0.0187
13	-0.5310	0.8474	0.0000	0.0182

14	0.0000	1.0000	0.0000	0.0192
15	0.5310	0.8474	0.0000	0.0182
16	-0.4690	0.7484	0.4690	0.0187
17	0.0000	0.8474	0.5310	0.0182
18	0.4690	0.7484	0.4690	0.0187
19	-0.4690	0.4690	0.7484	0.0187
20	-0.5310	0.0000	0.8474	0.0182
21	-0.4690	0.4690	0.7484	0.0187
22	0.0000	-0.5310	0.8474	0.0182
23	0.0000	0.0000	1.0000	0.0192
24	0.0000	0.5310	0.8474	0.0182
25	0.4690	-0.4690	0.7484	0.0187
26	0.5310	0.0000	0.8474	0.0182
27	0.4690	0.4690	0.7484	0.0187

Table 5. The results of non-uniform division (75 microplanes).

α	n_1^α	n_2^α	n_3^α	ω_a
1	0.6894	-0.5122	-0.5122	0.0070
2	0.7778	-0.5779	-0.2471	0.0065
3	0.8027	-0.5964	0.0000	0.0064
4	0.7778	-0.5779	0.2471	0.0065
5	0.6894	-0.5122	0.5122	0.0070
6	0.7778	-0.2471	-0.5779	0.0065
7	0.9122	-0.2898	-0.2898	0.0067
8	0.9531	-0.3028	0.0000	0.0068
9	0.9122	-0.2898	0.2898	0.0067
10	0.7778	-0.2471	0.5779	0.0065
11	0.8027	0.0000	-0.5964	0.0064
12	0.9531	0.0000	-0.3028	0.0068
13	1.0000	0.0000	0.0000	0.0070
14	0.9531	0.0000	0.3028	0.0068
15	0.8027	0.0000	0.5964	0.0064
16	0.7778	0.2471	-0.5779	0.0065
17	0.9122	0.2898	-0.2898	0.0067
18	0.9531	0.3028	0.0000	0.0068
19	0.9122	0.2898	0.2898	0.0067
20	0.7778	0.2471	0.5779	0.0065
21	0.6894	0.5122	-0.5122	0.0070
22	0.7778	0.5779	-0.2471	0.0065
23	0.8027	0.5964	0.0000	0.0064
24	0.7778	0.5779	0.2471	0.0065
25	0.6894	0.5122	0.5122	0.0070

*Only the data of the microplanes on the surface $\Gamma_{x=1}$ are presented here, however the data of the microplanes on the surface $\Gamma_{y=1}$ and $\Gamma_{z=1}$ can be obtained by permuting the directional cosine coordinates.

Now the grid on the surface of the cube is not uniform other than what shown in Figure 4. And the node coordinates in Equation (17) will be replaced with

$$\hat{r}_{ij} = (1, \eta_i, \eta_j), \quad (i, j = 1, 2, \dots, 2m) \quad (32)$$

However the method to calculate the normal vectors and the weights of all microplanes is still unchanged using Equations (20) and (21).

Calculate the directional cosines and weights of the improved microplanes, the results are shown in Table 4 and Table 5. Then figure out the non-uniform indicators of the microplanes in Table 4 and 5, and compare them with those in Table 1, 2, 3 and reference [3]. The result is given in Table 6,

which means that the distribution uniformity of the microplanes by means of non-uniform cubic surface grid method is improved greatly.

Table 6. The comparison of non-uniform indicators.

	N	$\max_{\alpha=1}^N \omega_\alpha$	$\min_{\alpha=1}^N \omega_\alpha$	λ_N
Table 1	21	0.0251	0.0199	25.80%
	33	0.0176	0.0099	78.37%
Ref. [1]	37	0.0211	0.0054	94.80%
	61	0.0100	0.0069	45.00%
Table 2	27	0.0319	0.0137	132.85%
Table 3	75	0.0122	0.0037	229.73%
Table 4	27	0.0192	0.0182	5.49%
Table 5	75	0.0070	0.0064	9.38%

6 CONCLUSION

In this paper, a new method, to generate microplanes by mapping regular grid of cubic surface onto the unit sphere surface, is proposed. Contrasting with the traditional methods, there are some advantages with the new method, such as that every microplane is clear in shape, so that the area covered by the microplane is distinct. It means that adaptive microplane refinement can be easily implemented, what needed for computing the weights of the refined microplanes is only to calculate the area of a spherical quadrilateral. The non-uniform indicator can be used to evaluate the distribution uniformity of the microplanes. It is indicated that, the weight distribution of the microplanes is non-uniform when the grid of cubic surface is meshed using uniform grid, however the uniformity of microplanes weight will be improved greatly for properly meshed non-uniform cubic surface grid.

ACKNOWLEDGEMENT

This paper is supported by the National Natural Science Foundation of China (Grant No. 90715022) and the Research Foundation of the State Key Laboratory of Disaster Resistance of Civil Engineering at Tongji University (SLDRCE 09-d-04).

REFERENCES

- Bažant, Z.P. and Oh, B.H. 1985, Microplane model for progressive fracture of concrete and rock[J]. Journal of Engineering Mechanics, ASCE: 111(4), 559-582.
- Bažant, Z.P. and Prat P C. 1988, Microplane model for brittle-plastic material I: theory[J]. Journal of Engineering Mechanics, ASCE, 114(10): 1672-1688.
- Bažant, Z.P., and Oh, B. H. 1985, Efficient Numerical Integration on the Surface of a Sphere Center for Concrete and Geomaterials, Northwestern University, Evanston Ill.,

- 1983; also Zeitschrift für Angewandte Mathematik und Mechanik (ZAMM), Leipzig, Germany, No. 83-2/428e.
- Bažant, Z.P., Caner F. C., Carol I. et al. 2000, Microplane model M4 for concrete I : formulation with work-conjugate deviatoric stress [J]. Journal of Engineering Mechanics, 126(9): 944-953
- Bažant, Z.P., Xiang Y., Prat P.C. 1996, Microplane model for concrete I : stress-strain boundaries and finite strain [J]. Journal of Engineering Mechanics, 122(3): 245-254
- I. Todhunter, M.A., F.R.S., 1863, Spherical Trigonometry, Cambridge and London, Macmillan and Co.
- State-of-the-art.1982, Finite Element Analysis of Reinforced Concrete. American Society of Civil Engineers, 345 East 47th Street New York, New York 10017.
- Taylor, G. I. 1938, Plastic strain in metals [J]. Inst. Metals, 62, 307-324.
- Zdenek P.Bažant and Ferhun C. Caner. 2005, Microplane model M5 with kinematic and static constraints for concrete fracture and anelasticity. I: Theory [J]. Journal of Engineering Mechanics, No. 41-47